Coherent and Clastic Rocks in the Southwest Zone Alkalic Porphyry Copper-Gold System, Galore Creek, Northwestern British Columbia (NTS 104G)

K. Byrne, Mineral Deposit Research Unit, University of British Columbia, Vancouver, BC (current address: Teck Corporation, Vancouver, BC, Kevin.Bryne@teck.com)

R.M. Tosdal, Mineral Deposit Research Unit, University of British Columbia, Vancouver, BC

K.A. Simpson, Mineral Deposit Research Unit, University of British Columbia, Vancouver, BC (current address: Geoscience BC, Vancouver, BC)

Byrne, K., Tosdal, R.M. and Simpson, K.A. (2010): Coherent and clastic rocks in the Southwest Zone alkalic porphyry copper-gold system, Galore Creek, northwestern British Columbia (NTS 104G); *in* Geoscience BC Summary of Activities 2009, Geoscience BC, Report 2010-1, p. 87–104.

Introduction

Calcalkalic porphyry deposits are well documented (Seedorff et al., 2005; Holliday and Cooke, 2007). In contrast, alkalic porphyry deposits are less well understood. Lang et al. (1995b, c), Jensen and Barton (2000) and Cooke et al. (2007) highlighted the economic significance of alkalic porphyry Cu-Au deposits and noted the subtle but significant differences from calcalkalic systems, as well as variations within the porphyry class itself. Alkalic porphyry Cu-Au deposits are known in only a few metallogenic terranes, notably the Triassic and Jurassic marine volcanic arcs of British Columbia (Barr et al., 1976; Lang et al., 1995c) and the Ordovician and early Silurian Lachlan Fold Belt in New South Wales, Australia (Cooke et al., 2007).

Galore Creek is an alkalic porphyry Cu-Au district located within the Stikine Terrane at the western margin of the Intermontane Belt in the Canadian Cordillera of northwestern BC (Figure 1). The interplay between breccia formation and mineralization events is integral to ore deposition in several BC alkalic porphyry systems, namely Mount Polley, Galore Creek, Copper Canyon and Crescent (Afton-Ajax area).The Southwest Zone Cu-Au breccia-centred deposit is one of 12 mineralized centres in the Galore Creek alkalic porphyry district and provides an important case study in the role of breccias in alkalic porphyry systems. Hosted in brecciated intrusive rocks that are distinctly younger than Central Zone Cu-Au mineralization (Schwab et al., 2008), the Au-rich Southwest Zone preserves late stages of magmatic-hydrothermal activity in the Galore Creek district (Enns et al., 1995; Schwab et al., 2008). This paper presents detailed coherent and clastic

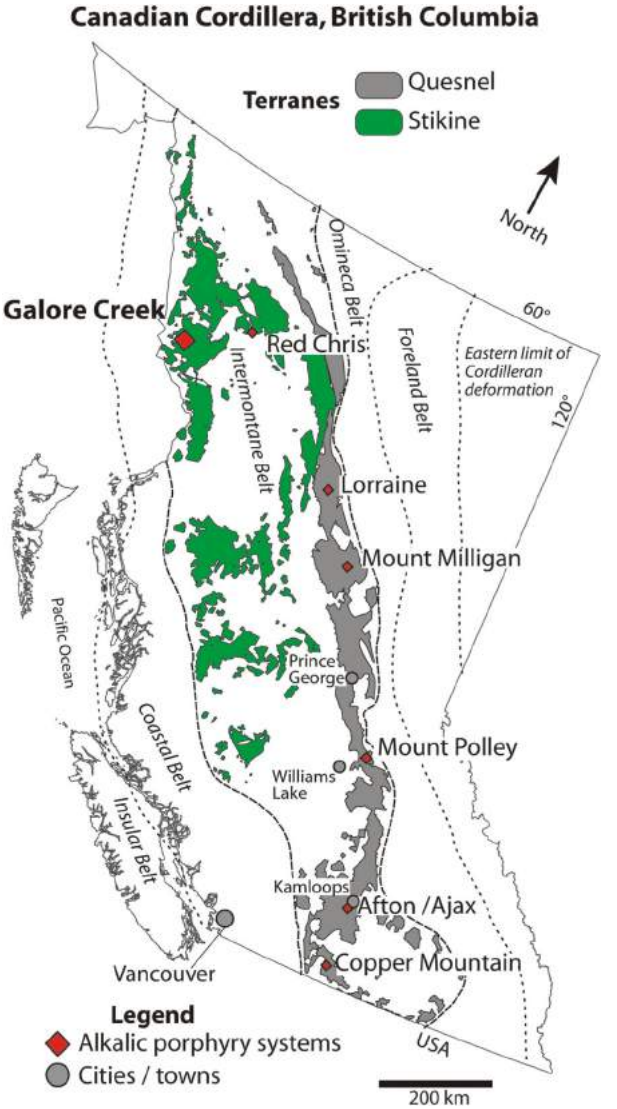

Figure 1. Mapped extent of the accreted Quesnel and Stikine ocean-arc terranes, major alkalic Cu-Au porphyry deposits and morphogeological belts. Galore Creek is located at the western margin of the Intermontane Belt, approximately 70 km east of Wrangell, Alaska. Data sourced from BC MapPlace (BC Geological Survey, 2010).

Keywords: *Galore Creek, breccia, intrusive rocks, alkalic porphyry*

This publication is also available, free of charge, as colour digital files in Adobe Acrobat® PDF format from the Geoscience BC website: http://www.geosciencebc.com/s/DataReleases.asp.

rock descriptions and parageneses in the Southwest Zone. The data presented are based on detailed drillcore logging of boreholes and a compilation of NovaGold Resources Inc. data on two cross-sections.

Regional Geological Setting

A collage of allochthonous oceanic and proximal to distal pericratonic terranes was accreted to the western margin of the North American craton during the Late Paleozoic to Late Mesozoic (Monger and Irving, 1980; Monger et al., 1982; Coney, 1989). McMillan (1991) grouped the Stikine, Cache Creek and Slide Mountain terranes, and parts of the Quesnel and Yukon-Tanana terranes into the Intermontane Superterrane. Quesnel and Stikine arcs host several alkalic intrusive centres and porphyry Cu-Au deposits of similar age (Figure 1), as well as calcalkalic porphyry Cu-(Mo-Au) deposits. Similarities in rock type and geological history between the Stikine and Quesnel terranes, including the presence of the silica-undersaturated alkalic porphyry deposits, have led workers to believe that they are segments of the same Triassic arc (Wernicke and Klepacki, 1988; Nelson and Mihalynuk, 1993; Mihalynuk et al., 1994). The alkalic Cu-Au deposits in both the Stikine and Quesnel terranes are products of two discrete alkalic magmatic events at the end of the Triassic and in the early Jurassic (Mortensen et al., 1995), and are interpreted to have formed outboard of ancestral North America in island-arc tectonic settings (McMillan, 1991).

District Geology

The Galore Creek alkalic intrusive suite is one of the largest and most silica-undersaturated complexes (Figure 2) to host porphyry Cu-Au deposits (Lang et al., 1995c). Galore Creek alkalic intrusions were emplaced between 210 ±1 and 200.1 ±2.2 Ma (Mortensen et al., 1995), and are hosted in supracrustal rocks of the Upper Triassic Stuhini Group (Figure 2B). Syenite, monzonite and monzodiorite stocks are hosted in rocks of shoshonitic affinity consisting of augite-phyric intermediate volcanic rocks, pseudoleucite-bearing phonolite and associated volcaniclastic rocks (Lang et al., 1995b, c). Kennecott Corporation defined a sequence of 12 intrusions for the Galore Creek alkalic intrusive suite (I1–I12; Enns et al., 1995), which is modified herein. The porphyry Cu-Au mineralization in the nearby Copper Canyon area is also hosted in alkalic intrusions (Bottomer and Leary, 1995).

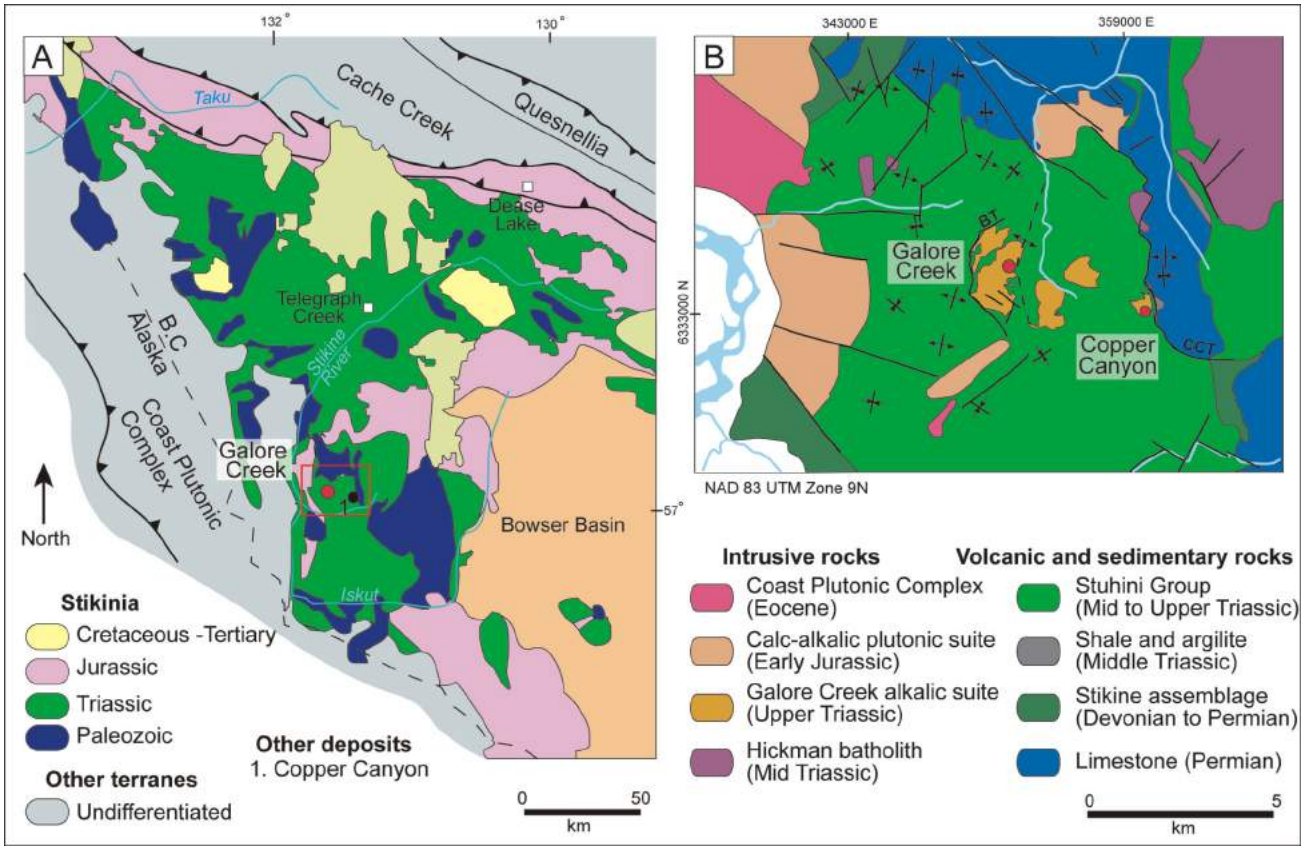

Figure 2. **A)** Major tectonostratigraphic elements of northwestern British Columbia (modified from Wheeler and McFeely, 1991; Gabrielse et al., 1991; Logan and Koyanagi, 1994) and location of the Galore Creek district (red dot) and Copper Canyon occurrence. The red box shows the location of Figure 2B. **B)** Regional-scale geology of Galore Creek district, showing the location of the Copper Canyon alkalic porphyry Cu-Au occurrence (modified from Logan and Koyanagi, 1994; Enns et al., 1995). Abbreviations: BT, Butte thrust fault; CCT, Copper Canyon thrust fault.

Hydrothermal alteration and mineralization are developed in the multiphase complex of alkalic intrusive and host shoshonitic volcano-sedimentary rocks. Twelve zones of Cu-Au mineralization are known (Figure 3). The largest deposit is the northerly-elongated Central Zone (Lang et al., 1995a; Micko et al., 2007; Schwab et al., 2008). Smaller prospects in the district include the Southwest Zone, Junction and North Junction, Butte, West Rim, Westfork and Saddle (Enns et al., 1995; Schwab et al., 2008). Two periods of hydrothermal activity, punctuated by intrusion of voluminous megacrystic orthoclase-phyric syenite and monzonite dikes, are known in the district (Schwab et al., 2008). Early mineralization occurs in the Central Zone and is hosted mostly in supracrustal rocks with subordinate Cu-Au in intrusions and hydrothermally cemented breccias. Mineralization in the Central Zone is truncated to the west by post-mineral, megacrystic, orthoclase-phyric syenite and monzonite dikes (Enns et al., 1995; Schwab et al., 2008). A second stage of mineralization is hosted in the same megacrystic orthoclase-phyric syenite and monzonite in the Southwest Zone (Figure 3), Middle Creek and Junction prospects (Schwab et al., 2008).

Three phases of deformation are recognized for the oldest Paleozoic rocks and one phase for Upper Triassic strata within the Stikine River–Iskut River region (Panteleyev, 1976; Logan and Koyanagi, 1994; Logan, 2004). The supracrustal rocks at Galore Creek are interpreted to have undergone early and broad-scale post-Triassic north-south compression followed by post–early Jurassic development of northerly-trending folds and thrust faults (Logan and Koyanagi, 1994), manifested by the post-mineral west-dipping Butte thrust fault (Schwab, et al., 2008) and the east-dipping Copper Canyon thrust fault (Bottomer and Leary, 1995). The deformation has tilted the Galore Creek district moderately (Byrne, 2009).

Rocks of the Southwest Zone

The Southwest Zone is situated ~600 m southwest of the South Gold lens in the southern part of the Galore Creek intrusive-volcanic complex (Figure 3), and is buried by glacial cover (Figure 4). The rocks of the Southwest Zone, based on relogging of drillcore, are divided into two groups: coherent and clastic. The coherent facies formed from the cooling and solidification of magma and is characterized by aphanitic or phaneritic textures. The clastic facies includes any fragmental rock; descriptions of these rocks follow McPhie et al. (1993). Characterization of clastic facies on the basis of infill types (matrix and cement) used criteria outlined by Davies et al. (2008b). Matrix, the fine-grained clastic component that occurs between larger clasts, comprises comminuted wallrock (rock flour), specifically lithic and crystal fragments of sand to granule size (<0.5–4 mm). Cement is a crystalline component within the clastic rock that precipitated from an aqueous fluid. Matrix-bearing breccias are clastic rocks with a component of matrix, with or without any additional cement. In the Southwest Zone, megacrystic orthoclase-phyric syenite and monzonite coherent-facies rocks are crosscut by matrix-bearing breccias, both of which host Cu-Au (Figure 4).

Coherent Rocks

Eight coherent rock types are recognized in the Southwest Zone (Table 1; Figure 5). Numerous dikes of intermediate to mafic composition crosscut all other rocks in the Southwest Zone and are considered unrelated to magmatism of the Galore Creek suite (Enns et al., 1995). The units are grouped as pre– or post–matrix-bearing breccia, based on observed and inferred crosscutting relationships. Of the eight coherent units, six are important to the evolution of the breccia (Figure 6). Three units are pre-breccia and three are post-breccia. The pre-breccia coherent rocks are as follows:

1) **Megacrystic orthoclase-phyric syenite** is characterized by tabular orthoclase (1–6 cm) and ~5% lath and equant orthoclase phenocrysts (0.2–1.0 cm) in a crystalline groundmass of K-feldspar, hornblende and biotite (Table 1, unit 2; Figure 6A). The unit occurs as thick (>100 m) composite dikes that intrude feldspar-phyric syenite (Table 1, unit 1).
2) **Megacrystic orthoclase- and plagioclase-phyric monzonite** is distinguished from other megacrystic units by plagioclase phenocrysts (Table 1, unit 3; Figure 6B). These megacrystic porphyries (units 2 and 3) host younger, less voluminous intrusions and are the dominant wallrock to clastic rocks (Figure 5).
3) **Acicular feldspar-phyric syenite** forms thin (0.5–3 m) dikes intruding the megacrystic porphyries (Table 1, unit 5; Figure 5.). Acicular-feldspar–phyric syenite is also a minor clast type in matrix-bearing breccia and locally displays irregular clast margins.

Post–matrix-bearing breccia coherent units are volumetrically minor and intrude megacrystic orthoclase-phyric syenite and monzonite, and clastic rocks. These include the following:

1) **Biotite-phyric monzodiorite** intrudes matrix-bearing breccia and is spatially coincident with much of the high-grade Cu-Au in the Southwest Zone (Table 1, unit 6; Figure 6C).
2) **Pyroxene-, hornblende- and biotite-phyric diorite** form dikes less than 2 m wide that cut cemented breccias. This unit locally contains minor Cu at its margins as veins and disseminations (Table 2, unit 7; Figure 6D).
3) **Orthoclase- and plagioclase-phyric monzonite** forms 1–5 m wide dikes that crosscut all breccia facies, are distinguished by characteristic glomeroporphyritic feld-

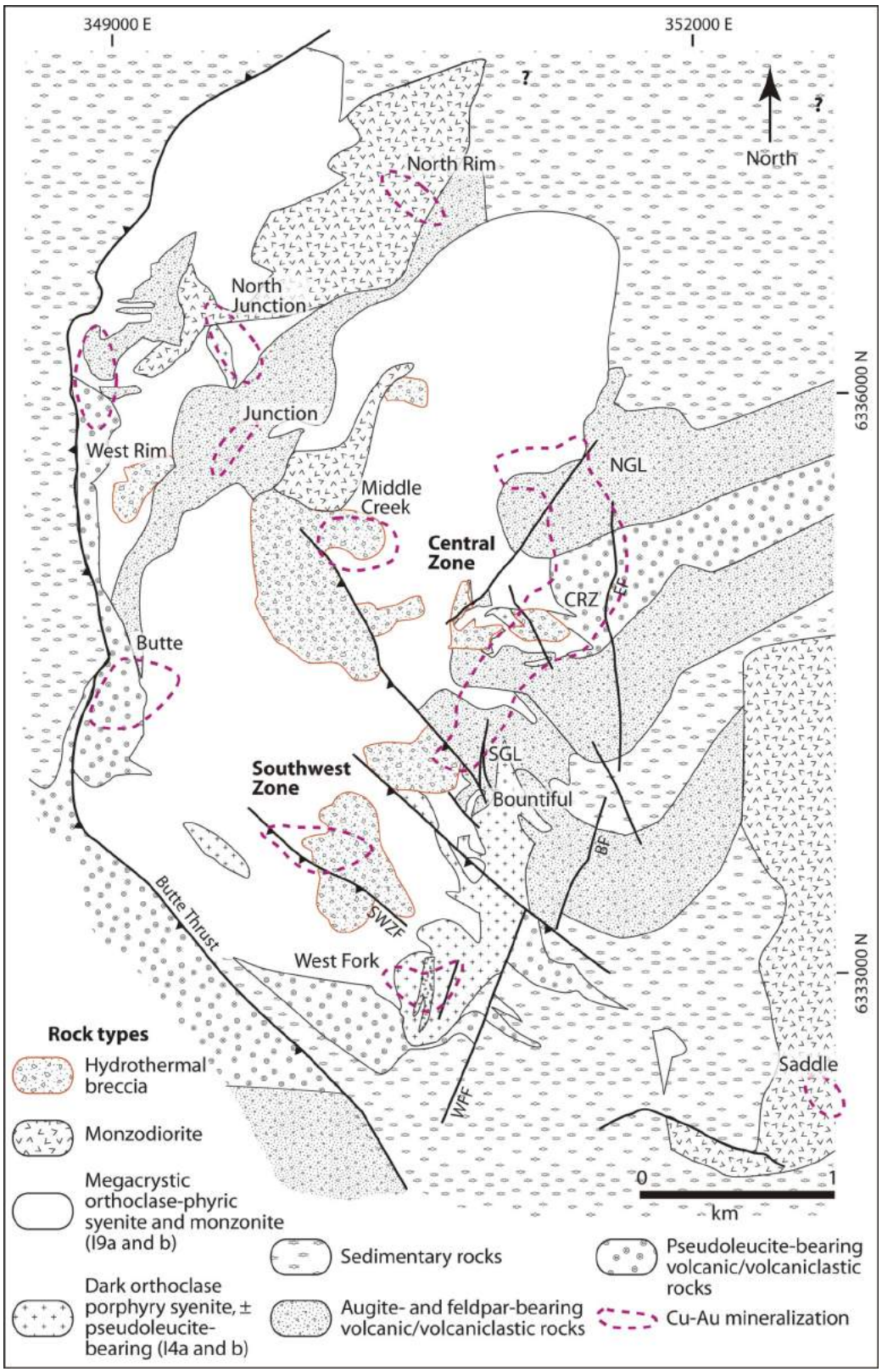

Figure 3. Simplified geology of the Galore Creek district, northwestern British Columbia, showing the location of mineralized centres and major structural features. Base map modified from maps of NovaGold Resources Inc., and rock type and distribution from drillhole and outcrop data. The names I9a, b and I4a, b refer to intrusive rock nomenclature used by Enns et al. (1995) and NovaGold Resources Inc. Abbreviations: NGL, North Gold lens; CRZ, Central Replacement zone; SGL, South Gold lens; SWZF, Southwest Zone fault; WFF, West Fork fault; BF, Bountiful fault; EF, East fault.

spar (Table 1, unit 8; Figure 6E) and postdate the Cu mineralization.

Biotite-phyric monzonite dikes are focused along the contact between the matrix-bearing breccia and porphyry wallrocks. Where it intrudes the matrix-bearing breccia, biotite-phyric monzodiorite forms volumetrically minor interconnected dikelets (Figures 7, 8). Fine-grained margins are observed within the biotite-phyric monzodiorite dikes; in contrast, the peripheral dikelet facies is characterized by irregularly shaped margins with local alignment of biotite phenocrysts (Figure 8). The dikelet facies may reflect peripheral fingering margins where it becomes disaggregated.

Clastic Rocks

There are three principal clastic facies in the Southwest Zone, based on the relative abundances of cement and matrix (Table 2):

1) matrix-bearing breccia with negligible cement (M-BX)
2) matrix-bearing breccia with 10–40% cement (matrix-dominated, MC-BX) and matrix-bearing breccia with >40% cement (cement-dominated, CM-BX)
3) cement-only breccia (C-BX)

The matrix-bearing breccia body is approximately 400 m wide by 800 m long, extends to at least 600 m below the surface and is discordant to the surrounding pre-fragmentation porphyry dikes. The western matrix-bearing breccia-wallrock contact, in its present geometry, is locally overhanging and trends broadly north and dips 60–70°W (Figures 4, 7). In contrast, the eastern contact is less well defined but appears to have a similar strike and dip. In plan view, the breccia body has an irregular oval shape elongated to the north (Figure 4). Section B–B' (Figure 7) cuts a steeply west-dipping overhanging protrusion of matrix-bearing breccia that results in the observed rollover of the wallrock contact from north to south. The northern and southern matrix-bearing breccia-wallrock contacts are not as well defined, although available drilling suggests the breccia body may continue south. Contacts between M-BX and wallrocks are described in Table 2.

Matrix-bearing breccia with no appreciable cement component (M-BX) is the most abundant breccia facies. Matrix-bearing breccia is predominantly polylithic, non-

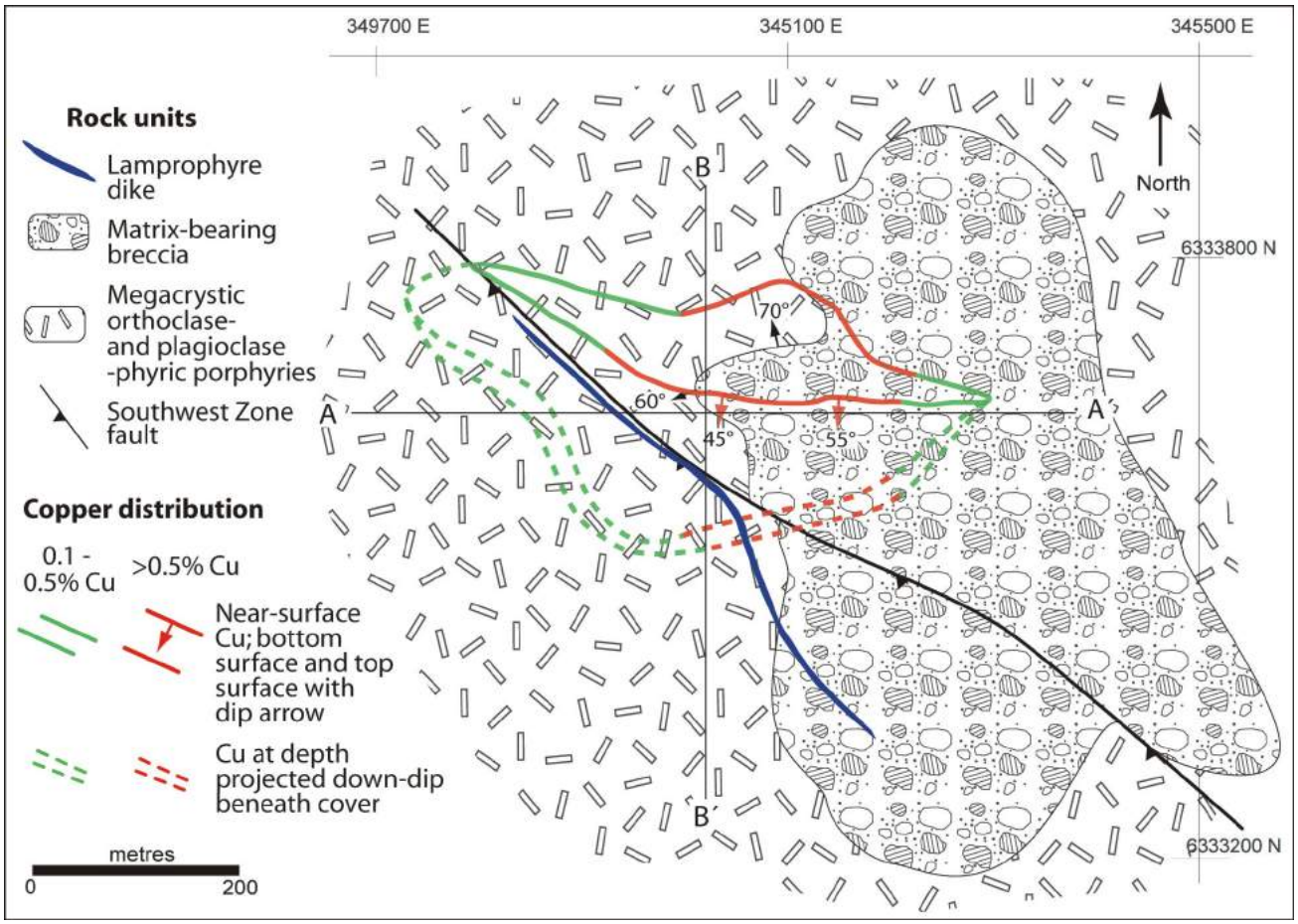

Figure 4. Simplified bedrock geology and Cu-grade distribution in the Southwest Zone, Galore Creek district, northwestern British Columbia, showing the locations of section lines A–A' (6333650N) and B–B' (350030E). Fire-assay data provided by NovaGold Resources Inc.

Table 1. Lithological characteristics of coherent rocks in the Southwest Zone, Galore Creek district, northwestern British Columbia.

Unit[1]	Coherent facies	Name[2]	Lithology description	Timing[3]
1	Feldspar-phyric syenite	I7	**Phenocrysts:** 1–2% lath and equant feldspars (0.5–1 cm). **Groundmass:** medium-grained equigranular. **Distinguishing features:** forms thick bodies with unclear geometries; appears to have variable phenocryst population containing some megacrysts	Pre
2	Megacrystic orthoclase-phyric syenite	I9A	**Phenocrysts:** 10–20% tabular orthoclase (1–6 cm) and ~5% lath and equant orthoclase (0.2–1.0 cm). **Groundmass:** medium-grained salt-and-pepper texture, 7–15% mafic minerals, 60% feldspar	Pre
3	Megacrystic orthoclase- and plagioclase-phyric monzonite	I9B	**Phenocrysts:** 5–20% tabular orthoclase (1–6 cm), 5–10% lath and equant orthoclase (0.2–1.0 cm), 20–35% lath and subhedral plagioclase (0.2–0.5 cm). **Groundmass:** medium-grained, 5% mafic minerals, 30–40% feldspar	Pre
4	Megacrystic orthoclase-phyric monzonite	I11	**Phenocrysts:** 5–15% lath to tabular orthoclase (0.5–2cm). **Groundmass:** medium-grained equigranular. **Distinguishing features:** trachytic orthoclase phenocrysts	Pre
5	Acicular-feldspar–phyric syenite	WFP	**Phenocrysts:** 5–25% acicular feldspar (0.2–1cm). **Groundmass:** dark, fine-grained. **Distinguishing features:** sometimes displays irregular clast margins; occurs throughout the matrix-bearing breccia body in minor amounts	Pre–syn?
6	Biotite-phyric monzodiorite	I6, I8B	**Phenocrysts:** 15–25% biotite (1–2 mm), ~3% hornblende needles (2–3 mm) and 60-70% feldspar. **Distinguishing features:** centred in the upper cemented breccia domain; typically mineralized by fine-grained chalcopyrite	Post
7	Pyroxene-, hornblende- and biotite-phyric diorite	V1 related dikes?	**Phenocrysts:** 5–10% hexagonal-shaped pyroxene (~0.2–0.8 cm), 5–10% biotite (booklets; 0.1–0.5 cm), >3% hornblende (0.2–1 cm) and 3–5% equant feldspar (0.2-0.4 cm). **Groundmass:** dark green, fine-grained. **Distinguishing features:** host to weak Cu mineralization	Post
8	Orthoclase- and plagioclase-phyric monzonite	I9(C)	**Phenocrysts:** 5–15% orthoclase (0.5–1.5 cm; rare megacrysts) and 10–25% anhedral plagioclase (0.2–0.6 cm). **Groundmass:** dark, fine-grained with 5–20% mafic minerals. **Distinguishing features:** glomeroporphyritic feldspar phenocrysts	Post
9[4]	Xenolith-bearing lamprophyre	D1	**Phenocrysts:** 10–20% biotite (0.1–0.2 cm) and 5–10% hornblende (0.3–0.5 cm). **Groundmass:** dark green, fine-grained	Post
10[4]	Mafic to intermediate dikes	D2-D3	**Phenocrysts:** 10% lath shaped feldspar (0.2–0.3 cm). **Groundmass:** fine-grained to aphanitic	Post

[1] Oldest to youngest units listed from top to bottom. Sequence of coherent rocks is based on observed and inferred crosscutting relationships.

[2] Name refers to intrusive rock nomenclature used by Enns et al. (1995) and references therein, and NovaGold Resources Inc.

[3] Timing is with respect to the formation of matrix-bearing breccia.

[4] Not part of the Galore Creek alkalic suite.

bedded, poorly sorted to chaotic (massive), matrix rich and matrix supported (Figure 9A, B). Clast to matrix ratio varies from 3:7 to 9:1 and averages approximately 7:3. Matrix is composed mostly of sand- and granule-size wallrock fragments (rock flour) with subordinate igneous biotite (Figure 9C) and feldspar crystals that may be derived from wallrock or possibly juvenile material. Fine-grained phlogopite±chlorite±magnetite is interstitial to granule-size lithic fragments (matrix) and gives the matrix a dark colour (Figure 9C, D). This fine phlogopite±chlorite±magnetite is observed throughout the matrix-bearing breccia body and may be composed of microcavity fill and alteration of clastic matrix. Clasts in matrix-bearing breccia are typically subrounded pebble to cobble size (Figure 9A, C). Cobble- to boulder-size monomict facies is proximal to the wallrock contact. Breccia margins are generally gradational over short distances but also locally abrupt or marked by dike intrusion. Sorting and stratification are evident over short intervals (5–10 cm) but are uncommon. Clasts in the matrix-bearing breccia are derived exclusively

from surrounding porphyry wallrocks. Acicular feldspar-phyric syenite occurs throughout the matrix-bearing breccia body in minor quantities and locally displays irregular clast margins (Figure 9D).

Numerous breccia clasts record older alteration and mineralization, as evidenced by alteration haloes (Figure 9A) and truncated K-feldspar and fine-grained biotite veins. Some of the pre-fragmentation alteration cannot be directly correlated to surrounding wallrocks, suggesting transportation of fragments from unobserved portions of the system. Pre-fragmentation porphyry dike contacts cannot be traced into the matrix-bearing breccia body, further demonstrating transportation of clasts away from the site of fragmentation.

A phlogopite±K-feldspar±anhydrite±magnetite±diopside±Cu-Fe–sulphide assemblage occurs as both hydrothermal cement and veins that cut the matrix-bearing breccia and host intrusions. Phlogopite and magnetite are the most common cement minerals associated with sulphides. Two spatially distinct cemented-breccia domains, an upper (main) and a composite lower, are present: (Figure 7). The upper cemented-breccia domain has a semi-ellipsoid morphology and is 20–100 m thick, 500 m wide and 400 m in length, tapering towards the tips. Cemented-breccia facies in this upper domain strike ~100°, dip 45–60°S and taper along strike. The lower cemented-breccia domain is characterized by multiple discontinuous cemented facies, 10–30 m thick. These lower cemented breccias are 10–30 m thick and have a geometry similar to those in the upper zone but poor continuity. Hydrothermal cement within the matrix-bearing breccias and older bordering wallrocks varies from negligible to abundant. Cemented-breccia facies are distinguished and mapped by the abundance and type of hydrothermal cement present (Table 2). Cement textures vary throughout MC-BX and CM-BX facies, irregular and straight-walled interconnected fracture fill that cuts both matrix and clasts (Figure 10A) through open-space fill between clast and matrix (Figure 10B–D) to irregularly shaped vugs. The MC-BX facies comprises <40% cement, with matrix making up the greater portion of the infill (Figure 10B, C). The CM-BX facies has >40% cement infill (Figure 10D–F).

Intrusive wallrocks contain in situ cemented breccia (coarse crackle-fracture) that lacks the matrix characteristic of other breccia facies (Figure 11A–C). In situ cemented breccia (C-BX) is both spatially and temporally contiguous with cement-dominated domains within the matrix-bearing breccia (Figure 7). Biotite-phyric monzodiorite dikelets are centred in MC-BX and CM-BX facies and are locally affected by cement, manifested as irregularly shaped vugs. Monolithic cemented breccia (C-BX) is also locally coincident with biotite-phyric monzodiorite dikelets (Figure 11A, B). The C-BX breccia facies is also typically very

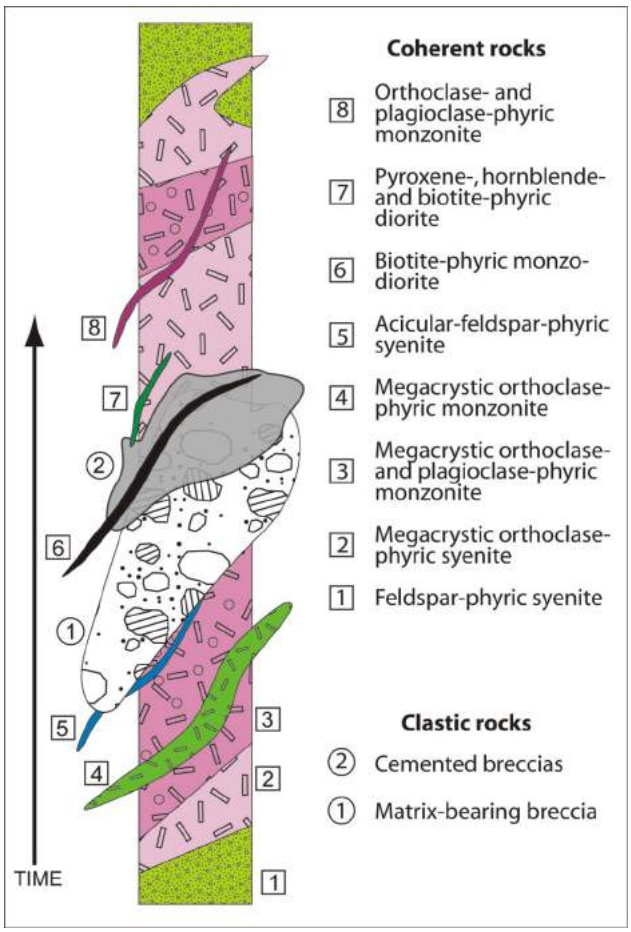

Figure 5. Sequence of coherent and clastic rock emplacement in the Southwest Zone, Galore Creek district, northwestern British Columbia.

coarse and displays a jigsaw-fit clast arrangement (Figure 11B, C). Clast morphology and organization in the polylithic matrix-bearing breccias suggests rotation and transport. In contrast, superposition of cemented-breccia facies (MC-BX, CM-BX and C-BX) shows little evidence of clast rotation or transport.

Evolution of Coherent and Clastic Rocks

Coherent and clastic rocks in the Southwest Zone are grouped into four paragenetic stages defined by their timing with respect to the fragmentation events associated with the formation of matrix-bearing–breccia and cemented-breccia facies (Table 3).

Feldspar-phyric syenite and megacrystic syenite and monzonite porphyry dikes are cut by matrix-bearing breccia. Acicular feldspar porphyry also occurs as clasts throughout the matrix-bearing breccia. However, some of these clasts display irregular margins, suggesting that the unit was incorporated prior to solidification, thus making it coeval with the matrix-bearing breccia. Therefore, the coherent units crosscut by the matrix-bearing breccia and

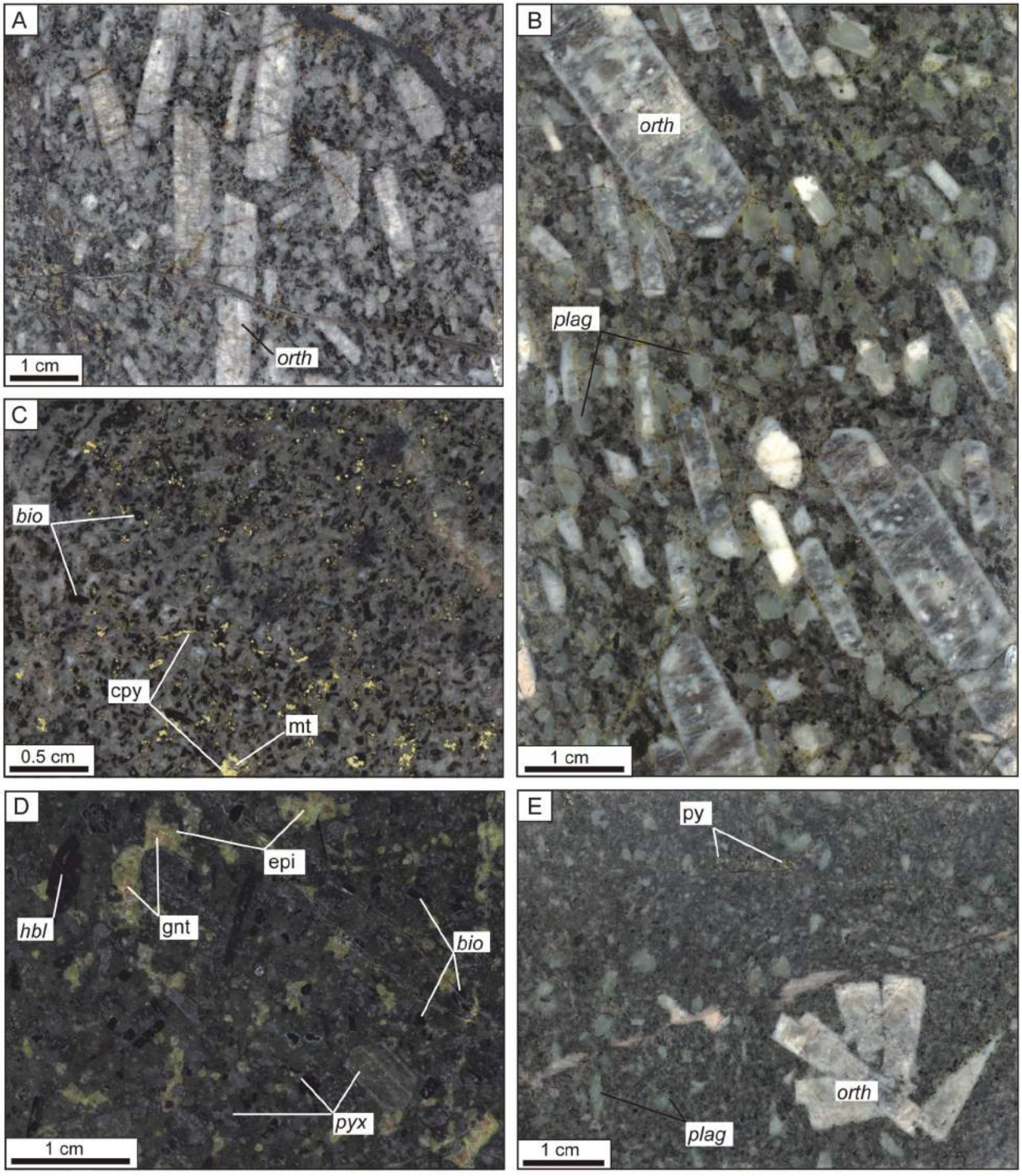

Figure 6. Photographs of coherent rocks in the Southwest Zone, Galore Creek district, northwestern British Columbia: **A)** megacrystic orthoclase-phyric syenite (unit 2); **B)** megacrystic orthoclase- and plagioclase-phyric monzonite dike (unit 3); **C)** biotite-phyric monzodiorite (unit 6); **D)** pyroxene-, hornblende- and biotite-phyric diorite; groundmass is pervasively chlorite altered (unit 7) and epidote-garnet forms clots in the groundmass; **E)** orthoclase- and plagioclase-phyric monzonite dike characterized by glomeroporphyritic orthoclase (unit 8). Abbreviations: bio, biotite; cpy, chalcopyrite; epi, epidote; gnt, garnet; hbl, hornblende; mt, magnetite; orth, orthoclase; plag, plagioclase; py, pyrite; pyx, pyroxene. Mineral abbreviations in italics refer to primary igneous minerals as opposed to alteration minerals.

acicular feldspar porphyry are grouped into stage 1 (Table 3).

Matrix-bearing breccia is superimposed by cemented breccia, locally resulting in the formation of MC-BX and CM-BX breccia facies (Figure 7). Concurrent with cement emplacement in matrix-bearing breccia, the cemented-breccia facies C-BX formed in adjoining coherent units. Cement emplacement is centred on and transects the older north-trending contact between matrix-bearing breccia and wallrock. Textural features and positions of biotite-phyric monzodiorite dikes and dikelets indicate that emplacement

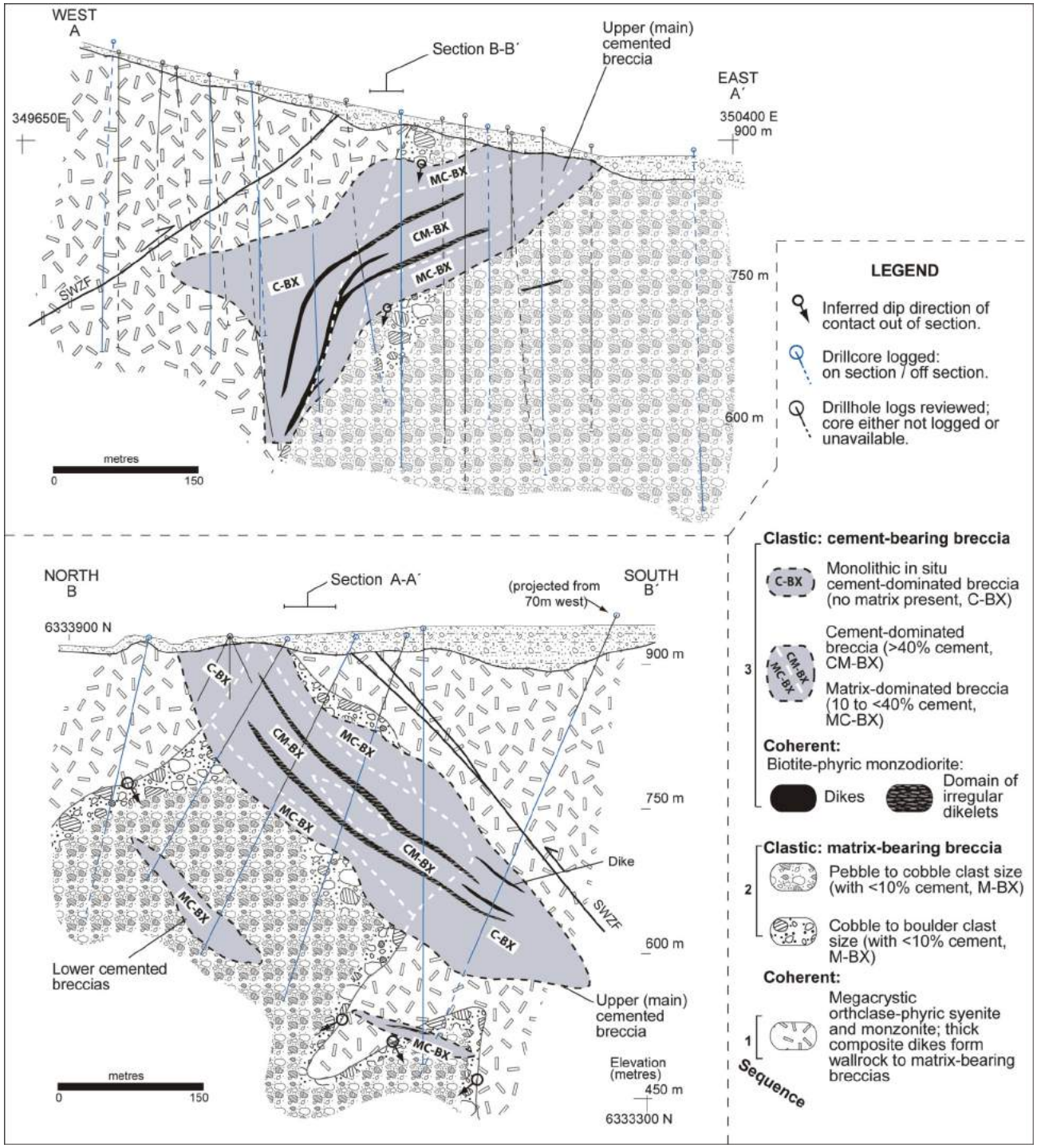

Figure 7. Distribution of clastic facies and simplified coherent facies along cross-sections A–A' (6333650N) and B–B' (350030E), Southwest Zone, Galore Creek district, northwestern British Columbia. See Figure 4 for location of section lines. Coherent-facies units 1, 4, 5, 7, 8, 9 and 10 are excluded from the figure for clarity. Drillhole data within 50 m of section A-A' and 40 m of section B-B' have been projected onto the respective sections. Abbreviation: SWZF, Southwest Zone fault.

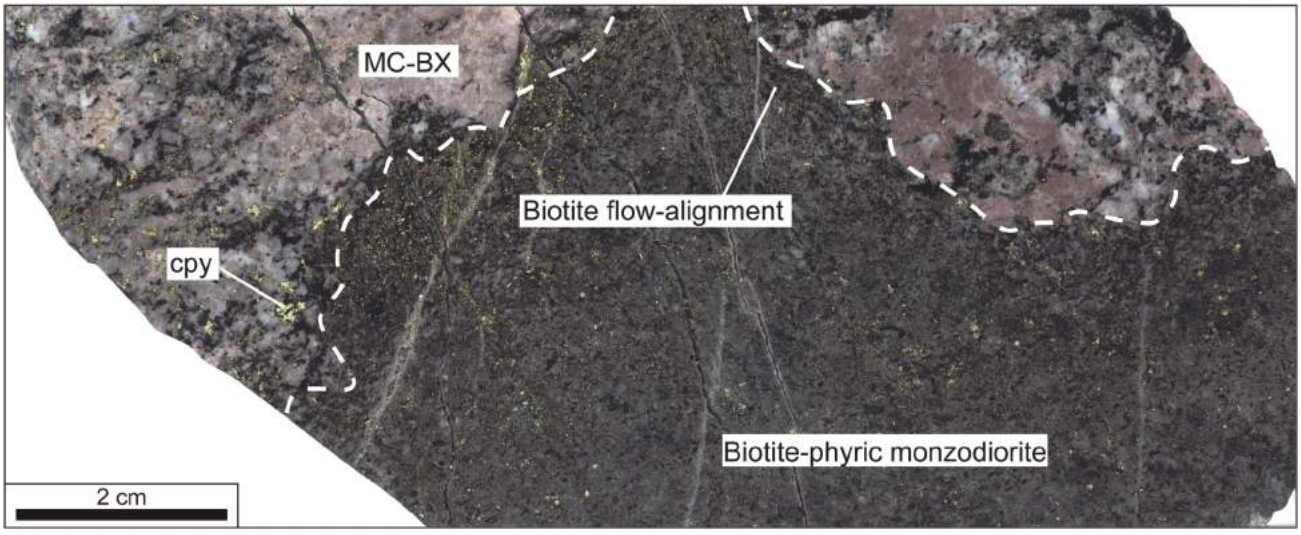

Figure 8. Biotite-phyric monzodiorite dikelet facies intrudes matrix-bearing breccia and exhibits weak flow fabric near the margins (dashed white line), Southwest Zone, Galore Creek district, northwestern British Columbia. Abbreviations: cpy, chalcopyrite; MC-BX, matrix-bearing breccias with 10–40% cement.

Table 2. Lithological characteristics of clastic rocks in the Southwest Zone, Galore Creek district, northwestern British Columbia.

Grouping	Clastic-facies nomenclature[1]	Infill proportion[2]	Cement/vein mineralogy[3]	Contacts	Lithology description
Matrix-bearing breccia with increasing cement component	M-BX: matrix-bearing breccia	<10% cement, ~90% matrix	phl, K-spar, diop, act, anh, mt, py, cpy	Sharp to gradational contact with wallrock marked by monolithic, very coarse facies	Predominantly polylithic, unbedded, unsorted to poorly sorted, matrix rich and matrix supported; clasts are subangular to subrounded and pebble to boulder size; clast to matrix Fractures, irregularly shaped veins and vugs are filled with varying proportions of cement minerals; sub-facies are distinguished by cement type and abundance; clast diameters commonly greater than drillcore width
	MC-BX: matrix-dominated breccia	10 to <40% cement, remainder is matrix	phl, K-Spar ± anh, mt, diop, cpy, bn	Gradational from weak stockwork veins and locally sharp	
	CM-BX: cement-dominated breccia	>40% cement, remainder is matrix	phl, K-Spar ± anh, mt, diop, cpy, bn	Over short distances CM-BX is transitional from MC-BX; sharp contact between CM-BX and M-BX also noted; late dikes typically occur proximal to cemented facies contacts	
Cement-only breccia	C-BX: monolithic in situ cement-dominated breccia	greater than ~90% cement, no appreciable matrix component	phl, K-Spar, diop, act, anh, mt, py, cpy, bn	C-BX facies is hosted in intrusive wallrocks and is contiguous with CM-BX and MC-BX; C-BX is transitional to weak stock-work veins	In situ or jig-saw–fit breccias are typically very coarse (large boulders)

[1] Clastic facies nomenclature and sub-facies refer to the scheme applied for sub-facies classification by cement mineralogy.
[2] Infill proportions refer to the amount of matrix and cement as proportions of total infill.
[3] Abbreviations: Abbreviations: act, actinolite; anh, anhydrite; bn, bornite; cpy, chalcopyrite; diop, diposide; K-spar, K-feldspar; mt, magnetite; py, pyrite; phl, phlogopite

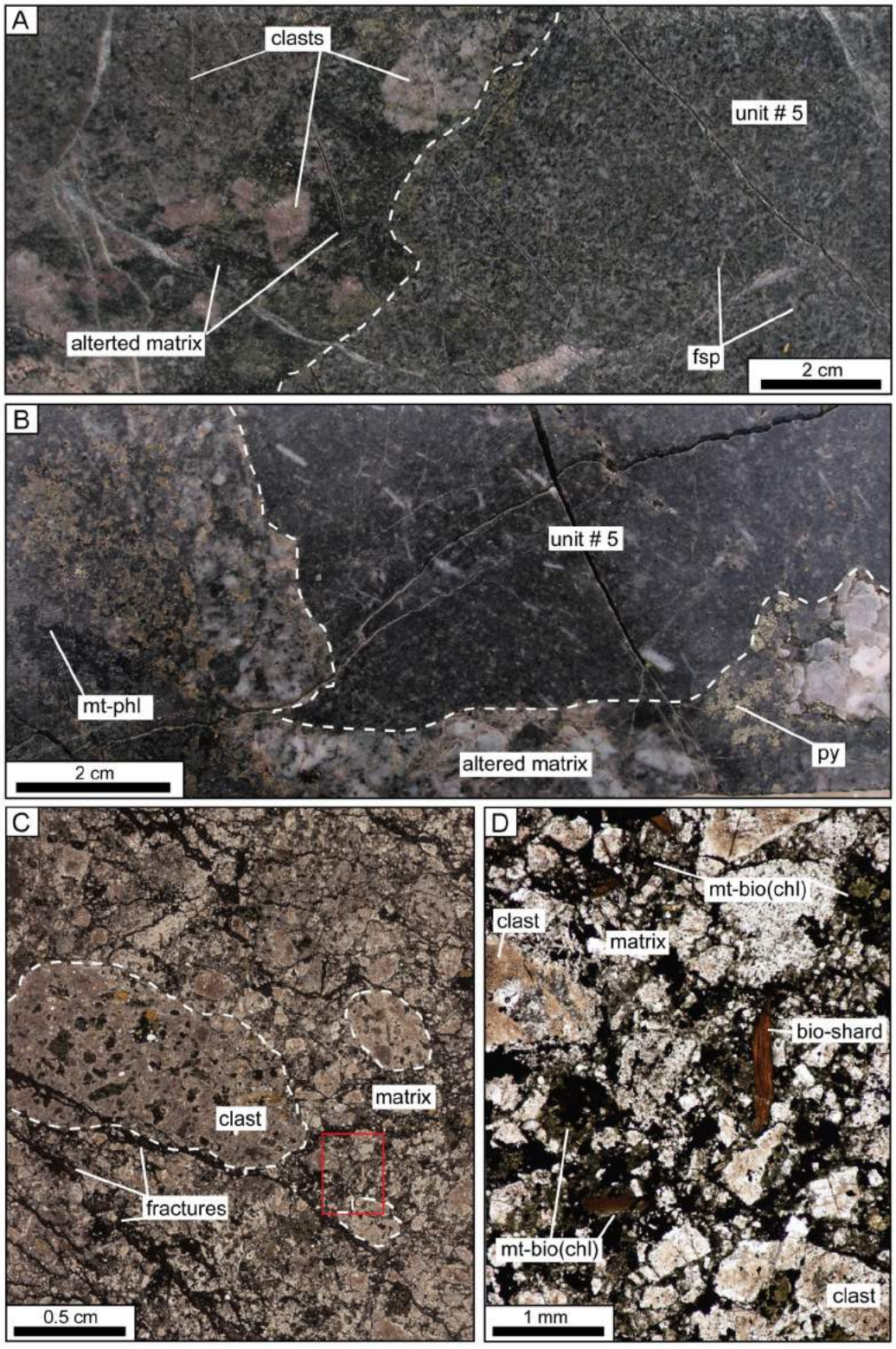

Figure 9. Photographs of diagnostic features in matrix-bearing breccias, Southwest Zone, Galore Creek district, northwestern British Columbia: **A)** polylithic M-BX with hematite–K-feldspar–altered cobble-size clasts and <10% cement; **B)** M-BX containing outsized clast of acicular feldspar-phyric syenite (unit # 5) with an irregular margin; **C)** thin-section scan in which some clasts are highlighted with dashed white lines; red box indicates the area expanded in the next photo; **D)** photomicrograph of matrix composed of sand- and granule-size fragments of wallrock (partially altered to magnetite-biotite and chlorite) and rare biotite crystals; note biotite crystal is not within a larger fragment. Abbreviations: bio, biotite; fsp, feldspar; mt, magnetite; phl, phlogopite; py, pyrite; pyx, pyroxene.

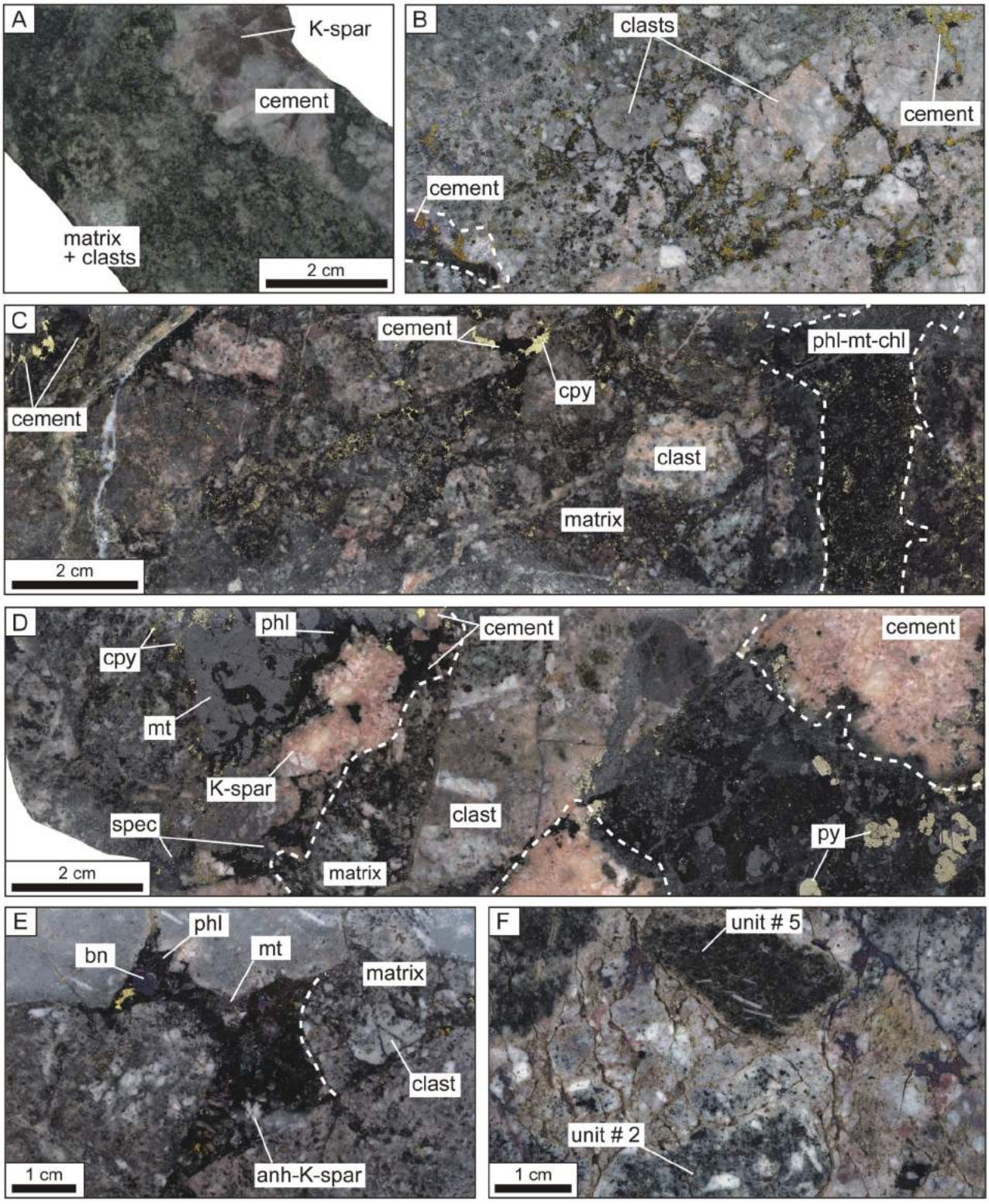

Figure 10. Photographs of cement-bearing breccia facies in the Southwest Zone, Galore Creek district, northwestern British Columbia: **A)** MC-BX, matrix-bearing breccia with <40 % cement; note the coarse K-feldspar cement; matrix is pervasively altered to chlorite-garnet; **B)** MC-BX, phlogopite-chalcopyrite–cemented breccia (highlighted by dashed white line); **C)** MC-BX, phlogopite-chalcopyrite±bornite±magnetite cement cuts matrix infill. **D)** CM-BX, cement-dominated breccia with >40% cement; note pervasive magnetite alteration of matrix (dashed white lines highlight boundaries between cement and matrix); **E)** CM-BX, phlogopite–bornite–chalcopyrite–magnetite–anhydrite–K-feldspar cement with subangular cobble-size clasts; **F)** CM-BX, K-feldspar–rich cement and alteration with bornite. Abbreviations: anh, anhydrite; bn, bornite; chl, chlorite; cpy, chalcopyrite; K-spar, K-feldspar; mt, magnetite; phl, phlogopite; py, pyrite; spec, specularite; unit # 2, megacrystic orthoclase-phyric syenite; unit # 5, acicular feldspar-phyric syenite.

was coeval with cemented-breccia formation. The cemented-breccia facies (MC-BX, CM-BX and C-BX) and biotite-phyric monzodiorite are therefore grouped together in stage 2.

The cemented-breccia facies is crosscut by multiple dikes, composed of pyroxene-, hornblende- and biotite-phyric diorite, and orthoclase- and plagioclase-phyric monzonite, which constitute stage 3 (Figure 12). Xenolith-bearing lamprophyre and several dikes of mafic to intermediate composition are not part of the Galore Creek alkalic suite, as defined by Enns et al. (1995), and are grouped as stage 4.

Structural Controls on Rock Distribution

Biotite-phyric monzodiorite dikes occur at the contact between the matrix-bearing breccia and porphyry wallrocks; dikelet facies occur in two discrete planar zones parallel to

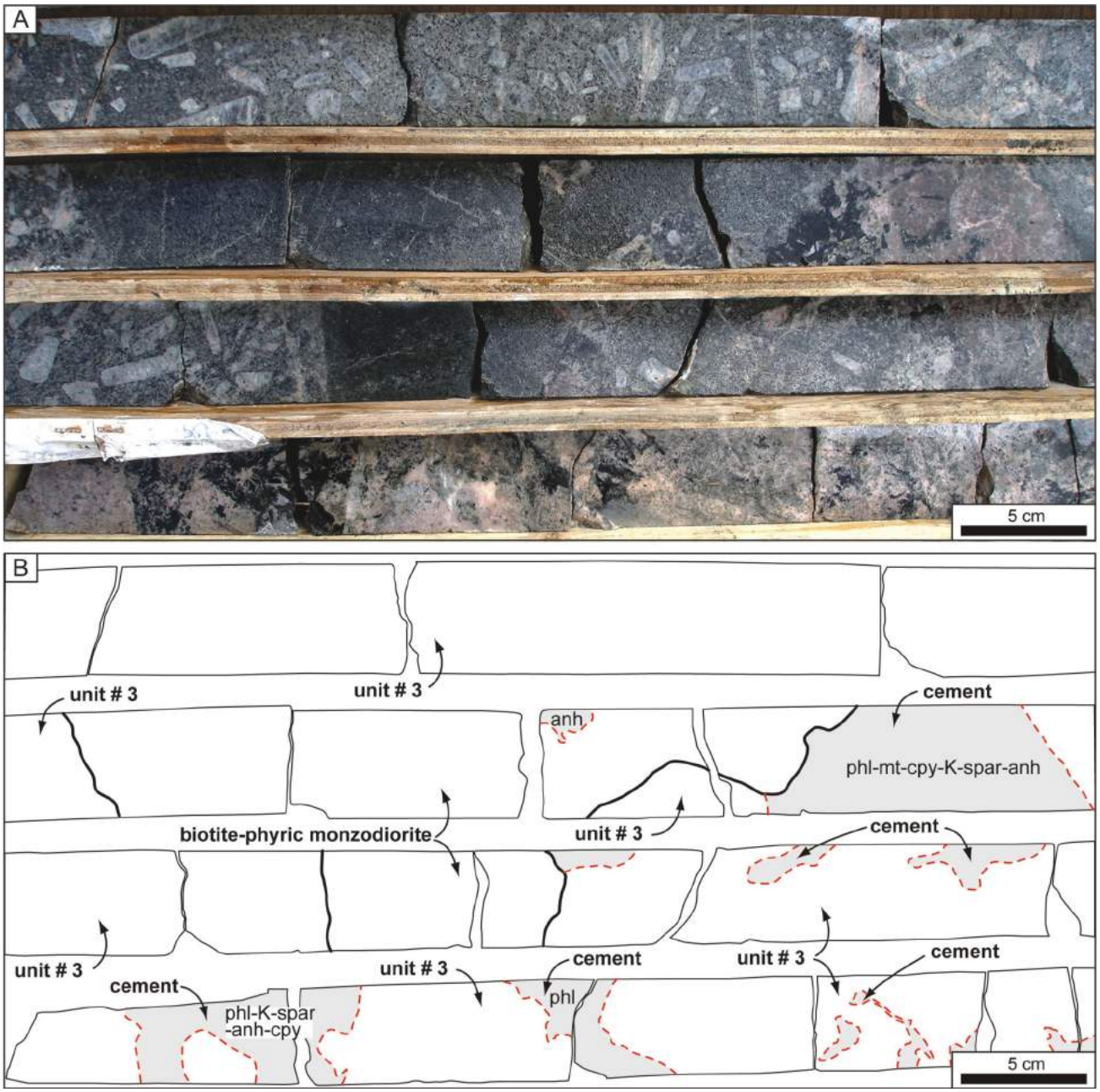

Figure 11. Photographs of monolithic, in situ cement-dominated breccias (C-BX): **A)** monolithic in situ cemented breccia (no matrix present; GC05-677, portions of core between 295.5 and 298.5 m); **B)** line traces illustrating pertinent features of drillcore shown in photo A; cemented domains highlighted with dashed red lines, and biotite-phyric dikelets marked with thick black lines and containing disseminated chalcopyrite and phlogopite alteration. Abbreviations: anh, anhydrite; cpy, chalcopyrite; K-spar, K-feldspar; mt, magnetite; phl, phlogopite; unit # 3, megacrystic orthoclase-phyric monzonite.

Table 3. Paragenetic stages of coherent and clastic rocks in the Southwest Zone, Galore Creek district, northwestern British Columbia.

Paragenetic stages[1]	Stage 1	Stage 2	Stage 3	Stage 4
Clastic rocks[2]	Matrix-bearing breccia	Cemented breccia		
Coherent rocks[3]	Units 1–5: feldspar-phyric syenite; megacrystic orthoclase-phyric syenite; megacrystic orthoclase- and plagioclase-phyric monzonite; megacrystic orthoclase-phyric monzonite acicular-feldspar-phyric syenite[4]	Unit 6: biotite-phyric monzodiorite[4]	Units 7 & 8: pyroxene-, hornblende- and biotite-phyric diorite; orthoclase and plagioclase-phyric monzonite	Units 9 & 10: xenolith-bearing lamprophyre; mafic to intermediate dikes

[1] Paragenetic stages are described in the text.
[2] Summary of clastic rock characteristics in Table 2.
[3] Summary of coherent rock characteristics in Table 1.
[4] Syn-breccia timing, paragenesis discussed in the text.

portions of the upper cemented-breccia domain (B–B'; Figure 7). The upper cemented-breccia domain is continuous along strike and down dip, whereas the lower domain is discontinuous, being composed of multiple discontinuous mineralized horizons (Figure 7). The cemented-breccia domains strike ~100°, dip 45–60°S and intersect the north-trending matrix-bearing breccia-wallrock contact. The planar geometry and along-strike and down-dip continuity of the cemented-breccia domains implies structural control on their formation. Furthermore, the ellipsoid geometry of the upper cemented-breccia domain is analogous to elliptical fault geometries (Peacock, 2002; Walsh et al., 2003). The geometric similarity of the cemented-breccia domains suggests they can be explained by a series of small nucleating faults that propagated into the matrix-bearing breccia and hydrothermal system.

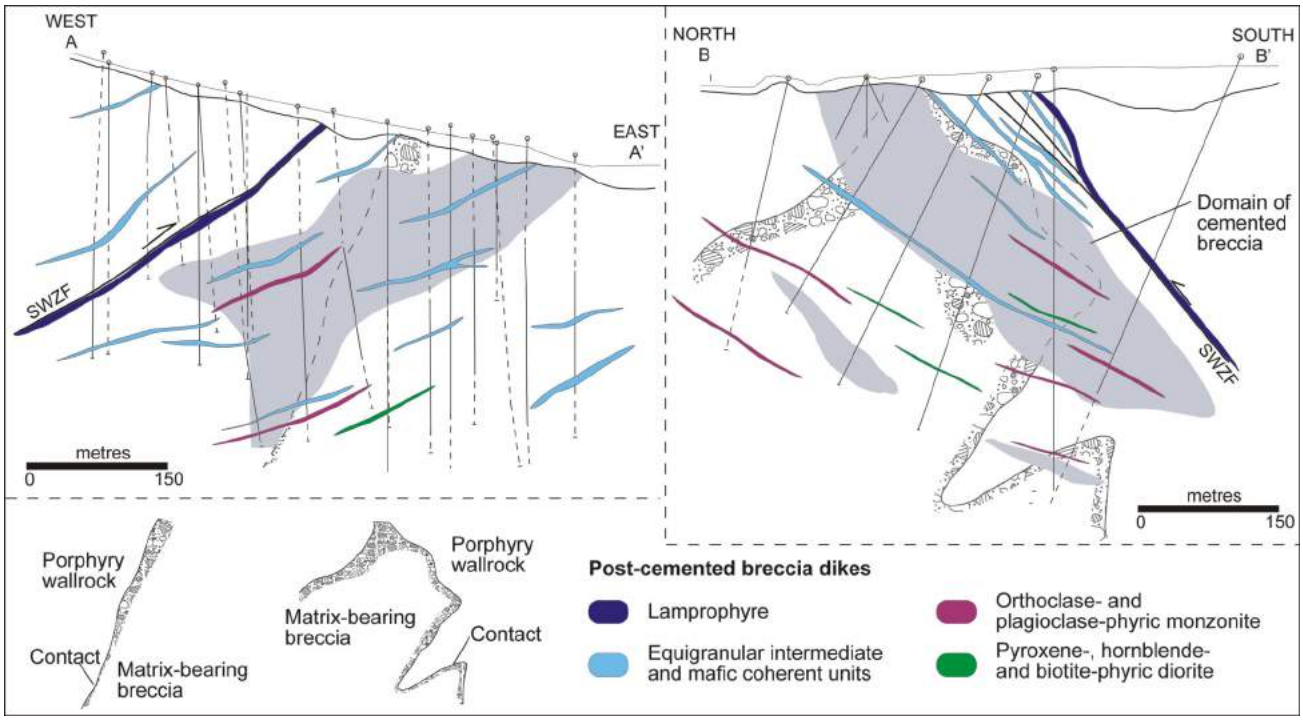

Figure 12. Post–cemented breccia facies coherent units. Abbreviation: SWZF, Southwest Zone fault.

Megacrystic porphyry units and breccias are cut by a post-mineral fault, the Southwest Zone fault (Figure 4). The fault strikes 120–130° and dips ~60°S, similar to reverse faults elsewhere in the district (Figure 3). A lamprophyre dike is locally coincident with this fault (Figure 4). The timing of lamprophyre emplacement, however, is ambiguous. Nonetheless, the extent and direction of displacement of coherent and clastic rocks shows a reverse separation of 200–250 m, although the true displacement is unconstrained. Post-mineral reverse separation along the Southwest Zone fault also locally truncates Cu-Au mineralization and alteration assemblages (Byrne, 2009).

Discussion and Genetic Interpretation

Matrix-Bearing Breccia

Key features of matrix-bearing breccia are as follows: 1) abundant fine-grained phlogopite-magnetite-chlorite alteration and microcavity fill in the matrix; 2) dominantly matrix rich and supported; 3) massive and poorly sorted; 4) polylithic, rounded to subrounded clasts of exclusively intrusive units; 5) moderately large areal extent (inferred from drillcore); and 6) hosted in porphyry wallrocks. Hydrothermal cement (stage 2) in the matrix-bearing breccia is the result of a younger superimposed event and is not directly linked to brecciation processes.

Matrix in the matrix-bearing breccia is pervaded by phlogopite-magnetite-chlorite as alteration and microcavity fill at most localities. The distribution, mineralogy and textural features of this alteration and microcavity infill suggest that magmatic-derived hydrothermal fluids dominated the environment synchronous with and post fragmentation. Fragment rounding and mixing, matrix (rock flour) generation and differential vertical displacement of fragments are all considered compatible with fluidization as a transport mechanism during the formation of subsurface breccias (McCallum, 1985; Sillitoe 1985). Unbroken phenocrysts in rock-flour–matrix breccias have been interpreted by Seedorff et al. (2005) as juvenile (tuffaceous) material. By analogy with Seedorff et al. (2005), biotite crystals in the matrix (Figure 9D), which do not appear to be part of a clast, are tentatively interpreted as a juvenile component. Moreover, delicate fluidal clasts are not unequivocally present, although acicular feldspar-phyric syenite locally displays irregular clast margins. These irregular margins suggest that the unit was incorporated into the breccia before solidification at some localities. Juvenile fragments and clasts with irregular margins suggest the presence of magma during fragmentation.

Based on their characteristics, matrix-bearing breccias in the Southwest Zone are interpreted to be the product of explosive fragmentation and primarily classified as hydrothermal (Sillitoe, 1985) or hydroclastic subsurface (Davies et al., 2008b) breccias. Explosive fragmentation is inferred to be the result of rapid expulsion of magmatic-hydrothermal fluids from cooling magma stocks (second boiling), coupled with decompression and liquid-vapour separation of already exsolved aqueous phases (Burnham, 1985; Sillitoe, 1985; Fournier, 1999). Juvenile material in the breccia suggests the presence of magma during fragmentation. In addition, fragmentation caused by steam expansion due to magma-fluid interaction (Sheridan and Woheltz, 1981; Hedenquist and Henley, 1985) is inferred to have produced juvenile material in the matrix. Overall, the evidence suggests that the matrix-bearing breccias were produced by a hybrid of fragmentation processes and can therefore be classified as magmatic-hydrothermal breccias with a subordinate phreatomagmatic component. Top and bottom terminations of the matrix-bearing breccia are not exposed in the present-day geometry and current erosion level. Therefore, it is unknown whether the magmatic-hydrothermal-phreatomagmatic explosions led to the disruption of rocks through to the paleosurface.

Cement-Bearing Breccias

Cement–bearing breccia facies (MC-BX, CM-BX and C-BX), veins and their associated alteration account for much of the Cu-Au budget in the Southwest Zone. Similar open-space filling, hydrothermally cemented breccias are widespread in porphyry systems and can be spatially associated with increased abundance of Cu-Au (Seedorff et al., 2005). Generally, hydrothermally cemented breccias form single or multiple lensoid, ovoid or circular pipe-like bodies with steep to vertical dips (Sillitoe, 1985; Seedorff et al., 2005).

At the Southwest Zone, the most abundant cement forms two subparallel horizons, the upper and lower cemented-breccia domains. Potassic cement minerals indicate moderately high temperature fluids of a dominantly magmatic source (Ulrich et al., 2001; Seedorff et al., 2005). Superimposition of hydrothermally cemented breccia facies on matrix-bearing breccias and porphyry wallrock is not associated with significant clast rotation or transport, implying that fragmentation was nonexplosive. Cement textures indicate emplacement by infill of 1) old and new fractures, 2) original open space between fragments in the matrix-bearing breccias, and by 3) open space generated by possible chemical corrosion or winnowing of matrix fines. Based on cement mineralogy and the environment of formation, cemented breccias are interpreted to be the result of nonexplosive fragmentation caused by the migration of magmatic-hydrothermal fluids. In this scenario, fragmentation of wallrock is the result of mechanical energy released during second boiling, decompression (Philips, 1972; Burnham, 1985) and subsequent hydraulic fracturing (Jébrak, 1997). Based on the inferred fragmentation mechanisms and criteria presented by Sillitoe (1985), Davies (2002) and Davies et al. (2008a), hydrothermally cemented

breccias in the Southwest Zone are interpreted as hybrid magmatic-hydrothermal-hydraulic breccias.

Root zones to the cemented breccias were not directly observed, although some magmatic-hydrothermal breccias are known to root in porphyry intrusions (Zweng and Clark, 1995; Jackson et al., 2007). Infill minerals, alteration and mineralization are centred on, and zoned about, cemented breccias and biotite-phyric monzodiorite facies. Distribution of infill and alteration facies, mineralization and metals are discussed below.

Evolution of the Southwest Zone Breccia Complex

The following model is proposed for the evolution of the Southwest Zone breccia complex, based on the above interpretations. Overpressure at the top of a hydrous magma chamber, due to second boiling, caused a rupture of magmatic-hydrothermal fluids and initiated explosive fragmentation. Fragmentation continued with decompression and was accompanied by subordinate phreatomagmatic explosions caused by the interaction of acicular feldspar-phyric syenite and water. Explosions propagated into megacrystic porphyry wallrocks, causing differential clast displacement, mixing and comminution that resulted in the formation matrix-bearing breccias. Ambient magmatic-hydrothermal fluids cemented microcavities (pore spaces) and altered clastic fines in the matrix-bearing breccias, greatly reducing porosity and permeability in matrix-rich facies.

Permeability regimes established post matrix-bearing breccia focused subsequent magmatic-hydrothermal fluids and strongly influenced the distribution of the cemented-breccia facies. The geometry of the upper and lower cemented-breccia domains suggests that structures played an important role in their genesis. An array of faults or fracture zones is interpreted to have intersected the matrix-bearing breccia-wallrock contact. The faults may have been dilatational features related to paleo–stress fields. Magmatic volatiles are inferred to have accumulated again in a cupola underlying the matrix-bearing breccias and subsequently expelled. The energy released during magmatic-hydrothermal fluid expulsion was sufficient to fracture the roof rocks but was not explosive. Decompression and hydraulic fracturing formed fluid channels that permitted access to the overlying rocks. Metal-bearing potassic fluids were preferentially channelled by the matrix-bearing breccia-wallrock contact and multiple intersecting fracture zones, with additional permeability generated by hydraulic fracturing. Fluid migration through newly formed fracture networks and the pre-existing permeability architecture resulted in formation of the cemented-breccia facies and Cu-Au zones.

Conclusions

Detailed drillcore logging and analyses of samples, on two cross-sections, has characterized the coherent and clastic rocks and their paragenesis in the Southwest Zone in the Galore Creek district of northwestern British Columbia. Matrix-bearing breccias and megacrystic porphyry units host Cu and Au mineralization centred in potassic, hydrothermally cemented breccias. The contact between matrix-bearing breccias and porphyry wallrocks served as the principal conduit and trap for ascending metal-bearing magmatic-hydrothermal fluids and biotite-phyric monzodiorite dikes. An array of faults intersecting this contact strongly influenced fluid-flow and the geometry of cemented breccias.

References

Barr, D.A., Fox, P.E., Northcote, K.E. and Preto, V.E. (1976): The alkaline suite porphyry deposits: a summary; *in* Porphyry Deposits of Canadian, A. Sutherland Brown (ed.), Canadian Institute of Mining and Metallurgy, Special Volume 15, p. 359–367.

BC Geological Survey (2010): MapPlace GIS internet mapping system; BC Ministry of Energy, Mines and Petroleum Resources, MapPlace website, URL <http://www.MapPlace.ca> [November 2010].

Bottomer, L.R. and Leary, G.M. (1995): Copper Canyon porphyry copper-gold deposit, Galore Creek area, northwestern British Columbia; *in* Porphyry Copper (± Au) Deposits of the Northern Cordillera, T. Schroeter (ed.), Canadian Institute of Mining and Metallurgy Special Volume 46, p. 645–649.

Burnham, C.W. (1985): Energy release in subvolcanic environments: implications for breccia formation; Economic Geology, v. 80, p. 1515–1522.

Byrne, K. (2009): The Southwest Zone breccia-centered silica-undersaturated alkalic porphyry Cu-Au deposit, Galore Creek, BC: magmatic-hydrothermal evolution and zonation, and a hydrothermal biotite perspective; M.Sc. thesis, Mineral Deposit Research Unit, University of British Columbia, 170 p.

Cooke, D.R., Wilson, A.J., House, M.J., Wolfe, R.C., Walshe, J.L., Lickfold, V. and Crawford, A.J. (2007): Alkalic porphyry Au-Cu and associated mineral deposits of the Ordovician to Early Silurian Macquarie Arc, New South Wales; Australian Journal of Earth Sciences, v. 54, p. 445–463.

Coney, P.J. (1989): Structural aspects of suspect terranes and accretionary tectonics in western North America; Journal of Structural Geology, v. 11, p. 117–125.

Davies, A.G.S. (2002): Geology and genesis of the Kelian gold deposit, East Kalimantan, Indonesia; Ph.D. thesis, University of Tasmania, 404 p.

Davies, A.G.S., Cooke, D.R., Gemmell, J.B., Leeuwen, T.V., Cesare, P. and Hartshorne, G. (2008a): Hydrothermal breccias and veins at the Kelian gold mine, Kalimantan, Indonesia: genesis of a large epithermal gold deposit; Economic Geology, v. 103, p. 717–757.

Davies, A.G.S., Cooke, D.R., Gemmell J.B. and Simpson K.A. (2008b): Diatreme breccias at the Kelian gold mine, Kalimantan, Indonesia: precursors to epithermal gold mineralisation; Economic Geology, v. 103, p. 689–716.

Enns, S.G., Thompson, J.F.H., Stanley, C.R. and Yarrow, E.W. (1995): The Galore Creek porphyry copper-gold deposits, northwestern British Columbia; *in* Porphyry Copper (± Au) Deposits of the Northern Cordillera, T. Schroeter (ed.), Canadian Institute of Mining and Metallurgy Special Volume 46, p. 630–644.

Fournier R.O. (1999): Hydrothermal processes related to movement of fluid from plastic into brittle rock in the magmatic-epithermal environment; Economic Geology, V. 94, p. 1193–1211.

Gabrielse, H., Monger, J.W.H., Wheeler, J.O. and Yorath, C.J. (1991): Morphogeological belts, tectonic assemblages, and terranes; *in* Geology of the Cordilleran Orogen in Canada, H. Gabrielse and C.J. Yorath (ed.), Geological Survey of Canada, Geology of Canada, no. 4, p. 15–28.

Hedenquist, J.W. and Henley, R.W. (1985): Hydrothermal eruptions in the Waiotapu geothermal system, New Zealand: their origin, associated breccias, and relation to precious metal mineralization; Economic Geology, v. 80, p. 1640–1668.

Holliday, J.R. and Cooke, D.R. (2007): Advances in geological models and exploration methods for copper ± gold porphyry deposits; *in* Proceedings of Exploration 07, B. Milkereit (ed.), Fifth Decennial International Conference on Mineral Exploration, Toronto, Ontario, p. 791–809.

Jackson, M., Tosdal, R.M. and Chamberlain, C.A. (2007): Igneous rocks related to brecciation and mineralization in the Mount Polley alkalic Cu-Au porphyry system, British Columbia; Arizona Geological Society, Ores & Orogenesis, Program with Abstracts, p. 166.

Jébrak, M. (1997): Hydrothermal breccias in vein-type ore deposits: a review of mechanisms, morphology, and size distribution; Ore Geology Reviews, v. 12, p. 111–134.

Jensen, E.P. and Barton, M.D. (2000): Gold deposits related to alkaline magmatism; Reviews in Economic Geology, v. 13, p. 279–314.

Lang, J.R., Lueck, B., Mortensen, J.K., Russell, J.K., Stanley, C.R. and Thompson, J.F.H. (1995a): Triassic–Jurassic silica-undersaturated and silica-saturated alkalic intrusions in the Cordillera of British Columbia: implications for arc magmatism; Geology, v. 23, p. 451–454.

Lang, J.R., Stanley, C.R. and Thompson, J.F.H. (1995b): Porphyry copper deposits related to alkalic igneous rocks in the Triassic–Jurassic arc terranes of British Columbia; *in* Porphyry Copper Deposits of the American Cordillera, F.W. Pierce and J.G. Bolm (ed.), Arizona Geological Society, Digest 20, p. 219–236.

Lang, J.R., Thompson, J.F.H. and Stanley, C.R. (1995c): Na-K-Ca magmatic hydrothermal alteration associated with alkalic porphyry Cu-Au deposits, British Columbia; *in* Magmas, Fluids and Ore Deposits, J.F.H. Thompson (ed.), Mineralogical Association of Canada, Short Course Series, v. 23, p. 339–366.

Logan, J.M. (2005): Alkaline magmatism and porphyry Cu-Au deposits at Galore Creek, northwestern British Columbia; *in* Geological Fieldwork 2004, BC Ministry of Energy, Mines and Petroleum Resources, Paper 2005-1, p. 237–248, URL <http://www.empr.gov.bc.ca/Mining/Geoscience/PublicationsCatalogue/Fieldwork/Pages/GeologicalFieldwork2004.aspx> [November 2009].

Logan, J.M. and Koyanagi, V.M. (1994): Geology and mineral deposits of the Galore Creek area, northwestern British Columbia (104G/3 and 4); BC Ministry of Energy, Mines and Petroleum Resources, Bulletin 92, URL <http://www.empr.gov.bc.ca/Mining/Geoscience/PublicationsCatalogue/BulletinInformation/BulletinsAfter1940/Pages/Bulletin92.aspx> [November 2009].

McCallum, M.E. (1985): Experimental evidence for fluidization processes in breccia pipe formation; Economic Geology, v. 80, p. 1523–1543.

McMillan, W.J. (1991): Tectonic evolution and setting of mineral deposits in the Canadian Cordillera; *in* Ore Deposits, Tectonics and Metallogeny in the Canadian Cordillera, BC Ministry of Energy, Mines and Petroleum Resources, Paper 1991-4, p. 1, URL <http://www.empr.gov.bc.ca/Mining/Geoscience/PublicationsCatalogue/Papers/Pages/1991-4.aspx> [November 2009].

McPhie, J., Doyle, M. and Allen, R. (1993): Volcanic textures: a guide to interpretation of textures in volcanic rocks; CODES Key Centre, University of Tasmania, 198 p.

Micko, J., Tosdal, R.M., Chamberlain, C.M., Simpson, K. and Schwab, D. (2007): Distribution of alteration and sulfide mineralization in the Central Zone of Galore Creek, northwestern British Columbia; Arizona Geological Society, Ores & Orogenesis, Program with Abstracts, p. 175.

Mihalynuk, M.G., Nelson, J.L. and Diakow, L.J. (1994): Cache Creek terrane: oroclinal paradox within the Canadian Cordillera; Tectonics, v. 13, p. 575–595.

Monger, J.W.H. and Irving, E. (1980): Northward displacement of north-central British Columbia; Nature, v. 285, p. 289–294.

Monger, J.W.H., Price, R.A. and Tempelman-Kluit, D.J. (1982): Tectonic accretion and the origin of two major metamorphic and plutonic welts in the Canadian Cordillera; Geology, v. 10, p. 70–75.

Mortensen, J.K., Ghosh, D.K. and Ferri, F. (1995): U-Pb geochronology of intrusive rocks associated with copper-gold porphyry deposits in the Canadian Cordillera; *in* Porphyry Copper (± Au) Deposits of the Northern Cordillera, T.G. Schroeter (ed.), Canadian Institute of Mining and Metallurgy Special Volume 46, p. 142–158.

Nelson, J.L. and Mihalynuk, M. (1993): Cache Creek ocean: closure or enclosure; Geology, v. 21, p. 173–176.

Panteleyev, A. (1976): Galore Creek map-area; *in* Geological Field Work, 1975, BC Ministry of Energy, Mines and Petroleum Resources, Paper 1976-1, p. 79–81, URL <http://www.empr.gov.bc.ca/Mining/Geoscience/PublicationsCatalogue/Fieldwork/Pages/GeologicalFieldwork1975.aspx> [November 2009].

Peacock, D.C.P. (2002): Propagation, interaction and linkage in normal fault systems; Earth-Science Reviews, v. 58, p. 121–142.

Philips, R. (1972): Hydraulic fracturing and mineralization; Journal of the Geological Society of London, v. 128, p. 337–359.

Schwab, D.L, Petsel, S., Otto, B.R., Morris, S.K., Workman, E. and Tosdal, R.M. (2008): Overview of the Late Triassic Galore Creek copper-gold-silver porphyry system; *in* Ores and Orogenesis, Circum-Pacific Tectonics, Geologic Evolution and Ore Deposits, J.E. Spencer and S.R. Titley (ed.), Arizona Geological Society, Digest 22, p. 471–484.

Seedorff, E., Dilles, J.H., Proffett, J.M., Einaudi, M.T., Zurcher, L., Stavast, W.J.A., Johnson, D.A. and Barton, M.D. (2005): Porphyry deposits: characteristics and origin of hypogene features; Economic Geology, 100th Anniversary Volume, p. 251–298.

Sheridan, M.F. and Wohletz, K.H. (1981): Hydrovolcanic explosions: the systematics of water-pyroclast equilibration; Science, v. 212, p. 1387–1389.

Sillitoe, R.H. (1985): Ore-related breccias in volcanoplutonic arcs; Economic Geology, v. 80, p. 1467–1514.

Ulrich, T., Gunther, D. and Heinrich, C.A. (2001): The evolution of a porphyry Cu-Au deposit, based on LA-ICP-MS analysis of fluid inclusions of fluid inclusions: Bajo de la Alumbrera, Argentina; Economic Geology, v. 96, p. 1743–1774.

Walsh, J.J., Bailey, W.R., Childs, C., Nicol, A. and Bonson, C.G. (2003): Formation of segmented normal faults: a 3-D perspective; Journal of Structural Geology, v. 25, p. 1251–1262.

Wernicke, B. and Klepacki, D.W. (1988): Escape hypothesis for the Stikine block; Geology, v. 16, p. 461–464.

Wheeler, J.O. and McFeely, P. (1991): Tectonic assemblage map of the Canadian Cordillera and adjacent parts of the United States of America; Geological Survey of Canada, Map 1712A, scale 1:2 000 000.

Zweng, P.L. and Clark, A.H., (1995): Hypogene evolution of the Toquepala porphyry copper-molybdenum deposit, Moquegua, southeastern Peru; *in* Porphyry Copper Deposits of the American Cordillera, F.W. Pierce and J.G. Bolm (ed.), Arizona Geological Society Digest, v. 20, p. 566–612.